Edinburgh Research Explorer

Chitinase-like proteins promote IL-17-mediated neutrophilia in a tradeoff between nematode killing and host damage

Chitinase-like proteins promote IL-17-mediated neutrophilia in a tradeoff between nematode killing and host damage

Tara E Sutherland[1], Nicola Logan[1], Dominik Rückerl[1], Alison A Humbles[2], Stuart M Allan[3], Venizelos Papayannopoulos[4], Brigitta Stockinger[4], Rick M Maizels[1] & Judith E Allen[1]

[1]Institute of Immunology and Infection Research, Centre for Immunity Infection and Evolution, School of Biological Sciences, University of Edinburgh, Edinburgh, UK. [2]Department of Respiratory, Inflammation & Autoimmunity, MedImmune, Gaithersburg, Maryland, USA. [3]Faculty of Life Sciences, University of Manchester, Manchester, UK. [4]Division of Molecular Immunology, Medical Research Council National Institute for Medical Research, London, UK. Correspondence should be addressed to J.E.A. (j.allen@ed.ac.uk) or T.E.S. (tara.sutherland@ed.ac.uk).

Enzymatically inactive chitinase-like proteins (CLPs) such as BRP-39, Ym1 and Ym2 are established markers of immune activation and pathology, yet their functions are essentially unknown. We found that Ym1 and Ym2 induced the accumulation of neutrophils through the expansion of γδ T cell populations that-produced interleukin 17 (IL-17). While BRP-39 did not influence neutrophilia, it was required for IL-17 production in γδ T cells, which suggested that regulation of IL-17 was an inherent feature of mouse CLPs. Analysis of a nematode infection model, in which the parasite migrates through the lung, revealed that the IL-17 and neutrophilic inflammation induced by Ym1 limited parasite survival but at the cost of enhanced lung injury. Our studies describe effector functions of CLPs consistent with innate host defense traits of the chitinase family.

Chitinase-like proteins (CLPs) are associated with a range of pathologies and are among the most abundant proteins found under conditions of type 2 activation of the immune system, but their functions remain poorly understood[1]. The CLPs are members of a family that include both chitotriosidase and acidic mammalian chitinase, enzymes that cleave chitin, which is a widespread structural component of arthropods, parasites and fungi. Consistent with the function of chitinases throughout the evolutionary tree[1], active chitinase enzymes act to defend the host against chitin-containing pathogens[2–4]. The CLPs, however, are catalytically inactive

due to loss-of-function mutations[5]. Evolutionarily recent gene-duplication events in mammals have resulted in expansion and diversification of the CLP-encoding genes such that each mammalian species exhibits a different array of CLP-encoding genes[5]. Mice have three CLPs (Ym1, Ym2 and BRP-39), while humans have two (YKL-39 and YKL-40). The rapid divergence of CLPs in mammalian species indicates a role for these proteins in host defense, but their expression patterns in many non-infectious settings[1,6] precludes the possibility that defense against pathogens is their sole function.

The mouse proteins Ym1 (encoded by *Chil3*) and Ym2 (encoded by *Chil4*) were the first CLPs to be identified as mediators of T helper type 2 (T_H2) inflammation in allergy[7,8]. Despite extensive publications describing increased expression of Ym1 during a wide range of pathologies, Ym1 is often disregarded as an important participant in CLP biology because of the lack of a true human ortholog of Ym1 and/or Ym2. Instead, emphasis has been placed on mouse BRP-39 (encoded by *Chil1*), which has the human homolog YKL-40 (encoded by *CHI3L1*). Studies of transgenic mouse models have shown that both BRP-39 and YKL-40 can contribute to the pathology of airway disease[9–12]. Because expression of all three mouse CLPs is upregulated in response to T_H2-driven inflammation in the lungs of mice, studying BRP-39 in isolation may not reveal the true functions of this closely related protein family.

We aimed to understand the general biology of CLPs by considering them as a family rather than by studying each in isolation. Our results revealed an unexpected role for Ym1 and, to some extent, Ym2 in driving the recruitment of neutrophils into the lungs, due to the ability of Ym1 and Ym2 to increase the number of $\gamma\delta$ T cells that expressed interleukin 17A (IL-17A). Although BRP-39 did not significantly influence neutrophil numbers, like Ym1 and Ym2, it did alter IL-17 expression in the models tested, which indicated that the ability to modulate IL-17 was a key feature of all three CLPs. We further demonstrated that the recruitment of neutrophils observed during the migration of *Nippostrongylus brasiliensis* through the lungs was mediated mainly by Ym1 in an IL-17-dependent manner. The Ym1-induced neutrophilia contributed to acute lung damage but, unexpectedly, Ym1 and IL-17 also impaired parasite survival. We thus highlight an anti-parasite effector mechanism by which Ym1 negatively influenced the integrity of parasites through IL-17-mediated recruitment of neutrophils but at a cost of increased lung damage.

RESULTS

Ym1 is the dominant CLP in the lungs

We examined the expression of *Chil1*, *Chil3* and *Chil4* in the lungs of BALB/c mice during T_H2 responses that resulted from ovalbumin (OVA)-induced allergic airway inflammation or during innate responses that were part of the acute lung injury caused by infection with *N. brasiliensis*. In the steady state, *Chil3* was the most abundant CLP-encoding transcript, followed by *Chil1* and *Chil4* (**Fig. 1a,b**). Despite being barely detectable in the lungs of mice challenged with PBS (**Fig. 1a**), *Chil4* was upregulated to the greatest degree after allergen challenge, followed by *Chil3* and finally *Chil4*, which showed limited change (**Fig. 1a** and **Table 1**). Similarly, at day 2 after infection with *N. brasiliensis*, *Chil4* was the only CLP-encoding gene that was significantly upregulated, as the increase in the expression of *Chil3* and *Chil1* was minimal (**Fig. 1b** and **Table 1**). Despite major differences between these models (allergy versus infection, and secondary responses versus innate responses), the pattern of CLP-encoding gene expression was strikingly similar. *Chil3* was the most abundant CLP-encoding transcript, *Chil4* exhibited the greatest change in expression but remained below *Chil1* and *Chil3*, and *Chil1* showed the least change in its expression.

Induction of CLP expression was also reflected at the protein level. Because of the high sequence homology between Ym1 and Ym2 (94%), there are no immunological tools that allow specific detection of Ym2 protein; instead, detection antibodies recognize both Ym1 and Ym2. We readily detected expression of CLPs in the lung in both airway epithelial cells and macrophages following allergen challenge, with the increased expression of Ym1 and/or Ym2 being visually more evident than changes to BRP-39 expression (**Fig. 1c**). Overall, our results describing gene and protein expression demonstrated that Ym1 and Ym2 were the dominant CLPs in the lungs of mice in terms of abundance and difference in expression, respectively.

Ym1 overexpression results in lung neutrophilia

All CLPs exhibited increased expression during lung pathology, yet the function of these molecules, particularly Ym1 and Ym2, remains elusive. Therefore, we developed an overexpression model to directly assess the function of Ym1, Ym2 and BRP-39. We administered plasmids encoding CLP sequences in a complex with polyethylenimine (PEI) intranasally to mice and monitored transfection by quantitative RT-PCR of lung tissue. As

expression peaked between 24 h and 48 h (data not shown), we chose 48 h as the time point for all subsequent analyses.

The number of macrophages containing microscopically observable particulate matter (corresponding to plasmid complexes) in mice that received the plasmid directly correlated with protein expression assessed by enzyme-linked immunosorbent assay (data not shown); thus, we used this as an indirect measure of transfection for all experiments. Approximately 35–40% of macrophages in the bronchoalveolar lavage (BAL) fluid contained complexes, independently of the plasmid administered (data not shown). To confirm selective overexpression, we measured the abundance of *Chil1* mRNA, *Chil3* mRNA and *Chil4* mRNA in total cells in BAL fluid. While transfection with empty vector did not alter the expression of CLP-encoding mRNA relative to naïve animals (data not shown), after transfection with CLP-encoding plasmids we found up to approximately 1000-fold specific overexpression of the relevant CLP-encoding mRNA (**Fig. 2a**).

We examined the composition of cells of the immune system in BAL fluid and lungs 48 h after plasmid administration and found that although the administration of CLP-encoding plasmids in complex with PEI did not change the abundance of total cells in the BAL fluid or lungs (**Fig. 2b**,**c**), neutrophil numbers were increased significantly following exogenous Ym1 expression (**Fig. 2d**–**f**). The absolute number of $CD4^+$ or $CD8^+$ T cells and $CD19^+$ B cells was not altered in the lungs of transfected mice, but eosinophil numbers were significantly reduced by exogenous Ym1 expression ($P < 0.05$ compared with vector only; analysis of variance (ANOVA) with Tukey-Kramer HSD multiple comparison test) (**Supplementary Fig. 1a–d**). Thus, exogenous expression of Ym1 in the lungs resulted in increased numbers of neutrophils and reduced numbers of eosinophils.

Ym1 neutralization reduces neutrophilia and IL-17

Specific inhibition of acidic mammalian chitinase markedly increases neutrophil numbers in the lungs, accompanied by increased Ym1 expression[13]. Our observation that exogenous Ym1 induced lung neutrophilia led us to speculate that the higher expression of Ym1 in allergic settings might contribute to the enhanced accumulation of neutrophils. To test this hypothesis, we used an OVA allergen model (**Supplementary Fig. 2**) and a mouse monoclonal antibody raised against a peptide in the Ym1 sequence that has been shown to be neutralizing[14].

Although the peptide sequence is derived from Ym1, there is a difference between Ym1 and Ym2 of only one amino acid and therefore the antibody may also have activity against Ym2.

We treated OVA-sensitized BALB/c mice with the antibody to Ym1 peptide (anti-Ym1) or immunoglobulin G2a (IgG2a) isotype-matched control antibody during aerosol challenge with either PBS or OVA (**Supplementary Fig. 2**) and assessed the recruitment of cells to BAL fluid. OVA challenge increased the number of total cells in the BAL fluid as well as the frequency of eosinophils and neutrophils among those cells (**Fig. 3a**). Allergic eosinophilia remained unaffected by treatment with anti-Ym1 (**Fig. 3a**), as did goblet-cell hyperplasia and the enhanced respiratory pause (data not shown). However, the frequency of neutrophils was reduced in OVA-challenged mice following treatment (**Fig. 3a**). Total neutrophil numbers were also reduced ($1.53 \times 10^5 \pm 0.24 \times 10^5$ neutrophils for IgG2a versus $0.91 \times 10^5 \pm 0.28 \times 10^5$ neutrophils for anti-Ym1 ($P < 0.05$, Students t-test; pooled from two independent experiments with 11–12 mice per group (mean ± s.e.m.)).

Both innate IL-17 production and adaptive IL-17 production are key processes involved in promoting the survival, recruitment and activation of neutrophils via regulation of target genes encoding cytokines and chemokines[15]. Although IL-17 is more typically associated with host defense against microbial infection, an important role for IL-17, and indeed neutrophils, during the pathogenesis of inflammatory lung diseases, including allergy and asthma, has emerged from research over the past decade[16]. Therefore, we investigated whether treatment of allergic mice with anti-Ym1 altered the expression of IL-17A as well as genes that are targets of IL-17. The secretion of OVA-specific IL-17A stimulated by anti-CD3 in splenocyte cultures was increased in allergic mice, a response attenuated by treatment with anti-Ym1 (**Fig. 3b**). Similarly the abundance of *Il17a* mRNA was significantly reduced in the lungs of allergic mice treated with anti-Ym1 (**Fig. 3c**), as was mRNA of the IL-17 target genes encoding the neutrophil chemotactic factors CXCL5 (*Cxcl5*) (**Fig. 3c**) and CCL3 (*Ccl3*) ($P < 0.01$, compared with treatment with OVA and IgG2a (analysis of variance (ANOVA) followed by Kruskal-Wallis test); data not shown). Thus, the allergic lung inflammation model suggested that Ym1 regulated neutrophil numbers through changes in the expression of IL-17A and genes that are targets of IL-17A.

γδ T cells are the source of IL-17A induced by CLPs

To determine whether the effects of Ym1 and Ym2 on IL-17 were lung specific or applied more broadly, we used the same transfection conditions as we used in studying the lungs (**Fig. 2**) and injected CLP-encoding plasmid, control plasmid or vehicle (5% glucose) into the peritoneal cavity. Approximately 20% of peritoneal macrophages and/or monocytes from transfected mice contained particulate matter corresponding to plasmid complexes (data not shown), and analysis of mRNA abundance in peritoneal cells revealed specific overexpression of each individual CLP-encoding mRNA (**Fig. 4a**). Of note, transfection with the plasmid encoding Ym1 increased the expression of both *Chil1* mRNA and *Chil4* mRNA (**Fig. 4a**), which suggested that members of the CLP family might have the ability to regulate each other.

Unlike the lung-transfection model, injection of plasmid into the peritoneal cavity caused significantly more accumulation of inflammatory cells than did injection of glucose alone (**Fig. 4b**). This probably reflected the uniquely high threshold of responsiveness to inflammatory stimuli in the lungs[17]. Nonetheless, the total number of peritoneal exudate cells (PECs) was higher following transfection with plasmid encoding Ym1 and Ym2 than after transfection with the control plasmid (**Fig. 4b**). While transfection in general increased the number of neutrophils, this effect was significantly enhanced when either Ym1 or Ym2 was overexpressed (**Fig. 4b**). The increased number of neutrophils was mirrored by an increase in *Il17a* expression in total PECs (**Fig. 4c**).

To identify the source of IL-17A following transfection with plasmid encoding Ym1 or Ym2, we stimulated total PECs *ex vivo* with the phorbol ester PMA plus ionomycin and stained intracellular IL-17A in the cells. Only a very small frequency of CD4$^+$ or CD8$^+$ T cells were IL-17A$^+$ (<2% of the T cell population; data not shown). Instead, γδ T cells constituted the major population of IL-17A-producing cells (**Fig. 4d**), and we detected no IL-17A in nonlymphoid cells of the peritoneal cavity (data not shown). The number of γδ T cells producing interferon-γ (IFN-γ) was not significantly altered by plasmid transfection (data not shown), but the proportion of IFN-γ$^+$ cells was reduced by overexpression of Ym1 or Ym2 (**Supplementary Fig. 3a**). Of note, transfection with plasmid encoding any of the CLPs resulted in more γδ T cells as well as IL-17A-producing γδ T cells than did transfection with control plasmid (**Fig. 4d,e**). We demonstrated that γδ T cells were the source of IL-17A following exogenous exposure to Ym1, not only in the peritoneal cavity but also in the lungs (**Supplementary Fig. 3b**).

Both IL-1β and IL-18 can act in synergy with IL-23 to stimulate γδ T cells to produce IL-17A[18], so we assessed the expression of these cytokines in PECs from transfected mice. While we did not detect mRNA encoding the p19 α-subunit of IL-23 (*Il23a* mRNA; called ' *Il23p19* mRNA' here) in PECs (data not shown), transfection with plasmid encoding Ym1 or Ym2 increased the expression of both *Il1b* and *Il18* (**Fig. 4f**,**g**). Overexpression of BRP-39 significantly increased the abundance of *Il18* mRNA but not that of *Il1b* mRNA (**Fig. 4f**,**g**), which might explain why BRP-39 had a lesser effect on IL-17A production than Ym1 and Ym2 (**Fig. 4c**,**e**),.

Because of the connection between IL-1β expression and the induction of IL-17-producing γδ T cells[18,19], we assessed whether blockade of the IL-1 receptor altered the effect of CLPs; for this we used anakinra, an antagonist of the IL-1 receptor[20]. Treatment with anakinra significantly reduced the ability of Ym1 to induce IL-17-producing γδ T cells in the peritoneal cavity (**Fig. 4h** and **Supplementary Fig. 3c**) and the accumulation of neutrophils in the peritoneal cavity (**Fig. 4i**). Of note, anakinra also prevented the suppression of IFN-γ following Ym1 overexpression (**Supplementary Fig. 3d**), which might have contributed to the enhanced IL-17 production in the presence of Ym1. Notably, the ability to suppress IFN-γ may be a general feature of Ym1, as treatment with anti-Ym1 elevates IFN-γ production by CD8+ T cells during coinfection with helminth and virus[21].

Along with subsets of γδ T cells, innate lymphoid cells (ILCs) are an important source of IL-17A that promote inflammation and immunity[22,23]. Analyzing the cellular composition of the peritoneal cavity, we detected a small population of IL-17A+ ILCs in both BALB/c wild-type mice and mice deficient in the recombinase component RAG-2 (**Supplementary Fig. 4a,b**). However, overexpression of Ym1 did not influence either the total number of ILCs or the number that expressed IL-17A (**Supplementary Fig. 4b**). Furthermore, Ym1 failed to recruit neutrophils into the peritoneal cavity of RAG-2-deficient mice (**Supplementary Fig. 4c**), which provided further evidence that γδ T cells rather than ILCs are the critical source of IL-17A. Collectively, our results suggested that Ym1 and Ym2 coordinated the recruitment of neutrophils *in vivo* by stimulating γδ T cells to produce IL-17A, via the induction of IL-1 and possibly IL-18. BRP-39 was also able to influence the number of IL-17A-producing γδ T cells in the peritoneal cavity (**Fig. 4d**,**e**), but this signal alone was not sufficient to substantially influence neutrophil recruitment in these models.

Ym1 contributes to *N. brasiliensis*–induced lung injury

Helminth infection induces strong T_H2 immunity. However, the initial acute response to the nematode *N. brasiliensis*, which migrates to the lungs, involves tissue damage, neutrophilic inflammation and hemorrhage[24]. Published work has highlighted not only the contribution of neutrophils to nematode-induced lung damage but also the role of alternatively activated macrophages in repairing that damage[24]. Since Ym1 is one of the molecules most abundantly produced by macrophages in this setting, it has been predicted to contribute to that repair. However, our unexpected finding that Ym1 induced neutrophilia suggested that Ym1 might instead contribute to acute lung injury. To investigate this, we infected BALB/c mice with 500 infective larvae of *N. brasiliensis* (third-stage larvae (L3)) and treated the mice systemically with either anti-Ym1 or isotype-matched control antibody. The number of neutrophils in BAL fluid (**Fig. 5a**) and lung tissue (**Fig. 5b**) was greater at day 2 following infection and lower by day 4. Consistent with our data obtained by transfection and for allergic airway inflammation, treatment with anti-Ym1 prevented the influx of neutrophils into the airways and treatment also reduced neutrophil numbers in the lung tissue at day 2 (**Fig. 5a**,**b**). The number of alveolar macrophages and lung interstitial macrophages in the BAL fluid was also reduced in infected mice at day 2 following treatment with anti-Ym1 compared with control antibody, an effect that was no longer apparent at day 4, at which point mice had not received antibody treatment for 72 h (**Fig. 5a**,**b**).

The changes in the number of neutrophils following treatment with anti-Ym1 were mirrored by a reduction in the expression of *Il17a* (**Fig. 5c**) and the IL-17A-target chemokine-encoding genes *Cxcl5* (**Fig. 5d**), *Ccl3* and *Cxcl1* (data not shown) in the lung tissue of mice at day 2 after infection. Additionally, the secretion of IL-17A from splenocytes stimulated ex-vivo with *N. brasiliensis* excretory secretory products at day 4 after infection was reduced by treatment with anti-Ym1 (**Supplementary Fig. 5a**), which suggested an altered adaptive IL-17 response to worm antigen. The expression of *Il23p19* increased in the lungs following infection but was not altered by treatment with anti-Ym1 (data not shown). However, as expected, *Il1b* mRNA expression in the lungs was attenuated by treatment with anti-Ym1 (**Fig. 5e**). Although the amount of IL-1β protein in whole-lung homogenates was significantly increased only at day 4 after infection in mice treated with IgG2a, treatment with anti-Ym1 reduced the abundance of IL-1β at day 2 relative to control antibody (**Fig. 5f**).

We next investigated whether the attenuated expression of IL-17A and reduced neutrophilia following treatment with anti-Ym1 affected acute lung injury. Histological assessment showed alveolar destruction and tissue hemorrhage at day 2 after *N. brasiliensis* infection and the initiation of repair and accumulation of inflammatory foci by day 4 (**Fig. 5g**). Treatment with anti-Ym1 diminished the tissue destruction observed at day 2 ($P < 0.01$, compared with treatment with OVA and IgG2a (analysis of variance (ANOVA) followed by Tukey-Kramer HSD multiple comparison test), as quantified by 'linear means intercept', a measurement of airspace enlargement. The effect of treatment with anti-Ym1 was no longer evident at day 4.

If Ym1 were acting via IL-17A, then IL-17A deficiency would mimic treatment with anti-Ym1 during the early stages of infection. To investigate this, we studied mice homozygous for insertion of a transgene expressing Cre recombinase into the endogenous *Il17a* gene (*Il17a*Cre) that were therefore deficient in IL-17A production and that also expressed enhanced yellow fluorescent protein (eYFP) from the ubiquitous *Rosa26* locus (*Rosa26*eYFP) as a reporter of Cre activity[25]. We infected those *Il17a*Cre*Rosa26*eYFP mice and C57BL/6 wild-type mice with 500 *N. brasiliensis* larvae (L3) and assessed their responses at days 2 and 4 after infection. At day 2, wild-type mice had the characteristic increase in the number of neutrophils in BAL fluid but, as expected, IL-17A-deficient mice failed to recruit neutrophils into the BAL fluid at day 2 after infection (**Fig. 6a**). Similar to published reports on the role of IL-17A during acute lung injury[24,26], IL-17A-deficient mice were protected from the peak of tissue damage following infection with *N. brasiliensis* at day 2 (**Fig. 6b**). However, despite the lower initial damage in the IL-17A-deficient mice, their lungs failed to repair appropriately by day 4, in contrast to the adequate repair in wild-type mice (**Fig. 6b**). This may have been related to our finding that in the absence of IL-17A, IL-13 production was also significantly diminished relative to wild-type mice (**Fig. 6c**). Notably, treatment with anti-Ym1 also prevented this early antigen-specific IL-13 response (**Supplementary Fig. 5b**).

Flow cytometry assessing intracellular IL-17A in wild-type mice allowed us to demonstrate that as in the peritoneal cavity, γδ T cells were a key source of IL-17A in the lungs of mice infected with *N. brasiliensis*. Very few IL-17A+ CD4+ or CD8+ T cells were present in their lungs and instead the majority of cells that expressed IL-17A were γδ T cells (**Fig. 6d,e**). We obtained similar results when we examined eYFP expression in lung-cell suspensions from

infected *Il17a*^{Cre}*Rosa26*^{eYFP} mice (**Supplementary Fig. 6**). Not only did we observe an increase in the number of IL-17A-secreting γδ T cells but also the absolute number of all γδ T cells was increased at both day 2 and day 4 following infection (**Fig. 6e**). Together these *N. brasiliensis* studies revealed that Ym1 induced IL-17A-producing γδ T cells, which, via IL-1, promoted the accumulation of neutrophils and thus contributed to acute lung injury associated with the migration of larvae through the lungs.

BRP-39 regulates IL-17 expression but not neutrophilia

Although overexpression of BRP-39 did not influence the number of neutrophils, it did result in enhanced IL-17A production in the peritoneal cavity and an increased number of IL-17-producing γδ T cells (**Fig. 4**). Because this overlapped with the observed effects of Ym1, we sought to determine whether the CLP family had common influences on IL-17A. We therefore infected *Chil1*^{−/−} mice and C57BL/6 wild-type mice with *N. brasiliensis* and assessed their responses at days 2 and 4 after infection. The abundance of *Il17a* transcripts in the lungs increased over the duration of infection in wild-type mice, as we had previously seen **(Fig. 5c)**. In contrast, we detected almost no *Il17a* mRNA in *Chil1*^{−/−} mice at day 2 and detected much less *Il17a* mRNA in *Chil1*^{−/−} mice than in wild-type mice at day 4 (**Fig. 7a**). Additionally, both the total number of γδ T cells and the number of IL-17A-producing γδ T cells were significantly lower in *Chil1*^{−/−} mice than in wild-type mice (**Fig. 7b**). Despite such differences in IL-17A-producing γδ T cells, there were no such observable differences in the number of lung neutrophils (**Fig. 7c**) or the expression of *Il1b*, *Il23p19* or *Il18* (**Fig. 7d**) or of *Cxcl5* or *Ccl3* (data not shown). Thus, not unexpectedly, there were no differences between *Chil1*^{−/−} mice and wild-type mice in terms of tissue damage (data not shown).

Ym1 contributes to innate anti-nematode defense

Our data demonstrated that neutralization of Ym1, depletion of neutrophils or IL-17 deficiency during infection with *N. brasiliensis* limited acute lung injury, results supported by published studies of the roles of neutrophils and IL-17 (refs. 24,27). However, the diminished neutrophilia and resultant lung injury could have reflected changes in the number of larvae that reached the lung. We therefore assessed the expression of *N. brasiliensis*–specific actin-encoding mRNA in whole lungs. While such a measurement cannot distinguish between live larvae and dead larvae, it did indicate that at day 2 after infection, at the peak of lung injury, a similar number of

larvae had entered the lungs of mice treated with isotype-matched control antibody or anti-Ym1 (**Fig. 8a**), as well as IL-17A-deficient mice (**Fig. 8b**) and *Chil1*$^{-/-}$ mice (**Fig. 8c**). Therefore, the differences in neutrophilia and acute lung injury could not be explained by a reduction in the number of worms that reached the lungs.

We additionally assessed worm burden in the small intestine at day 4 after infection. The data showed that treatment with anti-Ym1 increased the number of larvae reaching the gut by approximately twofold compared to control antibody treatment (**Fig. 8d**). IL-17A-deficient mice also exhibited an increased worm burden in the small intestine at day 4 relative to wild-type mice (**Fig. 8e**), with a phenotype similar to that resulting from blockade of Ym1 (**Fig. 8d**). Despite the lower amount of IL-17A production in *Chil1*$^{-/-}$ mice infected with *N. brasiliensis* as compared to infected wild-type mice, we observed no differences in worm burden (**Fig. 8f**), which suggested a role for neutrophils in resistance to parasites. The possibility of a role for neutrophils in the assault on the parasite was supported by histological analysis of neutrophils in the lungs of mice treated with anti-Ym1 versus those treated with isotype-matched control antibody (**Fig. 8g**). In lung sections of all mice, we observed organized 'swarms' of neutrophils around larvae, but the number of neutrophil swarms (**Fig. 8h**) and their size (**Fig. 8i**) was significantly reduced in mice treated with anti-Ym1 relative to treatment with the isotype control. Frequency distribution analysis further illustrated that not only did mice treated with anti-Ym1 have fewer swarms than did mice treated with isotype-matched control antibody but also those swarms contained only 50–100 neutrophils and did not achieve the large number of neutrophils seen in the control mice (**Fig. 8j**). To provide further evidence that Ym1 was sufficient to enhance parasite resistance, we transfected mice with plasmid encoding Ym1 to increase protein abundance and the number of neutrophils in the lungs before infection with *N. brasiliensis* larvae (L3). The number of parasites was significantly reduced in the intestines of mice in which Ym1 was overexpressed in the lungs as compared to mice transfected with the empty vector (**Fig. 8k**). Of note, the difference between mice given pcDNA3.1 and those given plasmid encoding Ym1 in terms of parasite recovery increased as the worms migrated through the intestine (**Fig. 8l**), which suggested that exposure to Ym1 and neutrophils in the lungs had compromised the fitness of the parasite. Overall, the increase in the number of parasites in the gut demonstrated that Ym1 and IL-17A were involved in limiting parasite burden (probably through actions on neutrophils), but at the cost of enhanced lung damage (**Supplementary Fig. 7**).

DISCUSSION

Neutrophils and the T_H17 subset of helper T cell are regarded as important inflammatory cells in patients with chronic severe asthma or steroid-resistant asthma[28–30], and expression of the human CLP YKL-40 is increased during chronic obstructive pulmonary disease[31] and active colitis[32], conditions that are also associated with responses by T_H17 cells and neutrophils[33,34]. YKL-40 expression in children with severe, steroid-resistant asthma or patients with cystic fibrosis correlates with neutrophil abundance [11,35], which contributes to the notion that CLPs regulate neutrophilic inflammation during pathology. Our studies with direct transfection demonstrated the ability of all three mouse CLPs to induce the expansion of IL-17-producing γδ T cell populations. In support of a model in which regulation of the IL-17 pathway is an inherent feature of the mouse CLP family, both *Chil1*$^{-/-}$ mice and mice treated with anti-Ym1 failed to upregulate their expression of *Il17a* mRNA in the lungs at day 2 following infection with *N. brasiliensis*. Unlike the effect of Ym1, the influence of BRP-39 in these settings was not sufficient to influence the number of neutrophils. Notably, our findings are consistent with studies showing a correlation between IL-17A expression and the expression of both BRP-39 and Ym1 (refs. 36,37).

From an evolutionary standpoint, a role for enzymatically inactive CLPs in innate immunity is not altogether unexpected, given that their close 'relatives' contribute to immunological defense through the degradation of chitin from invading pathogens[38] and BRP-39 has been shown to contribute to defense against *Streptococcus pneumonia*[36]. Here we found that Ym1 and Ym2, through the regulation of IL-17-producing γδ T cells and neutrophils, served a crucial host-protective role by limiting nematode burden. Notably, γδ T cells are similarly triggered to produce IL-17A following the administration of chitin in the lungs[19], but the involvement of CLPs was not explored in those studies. While control of helminth infection is typically dependent on T_H2 immunity[39], there is growing evidence that neutrophils contribute to killing nematodes[40,41]. Of note, Ym1 enhanced not only the number of neutrophils in the lung at day 2 after infection but also the number of alveolar and interstitial macrophages. Therefore, Ym1 might control parasite worm burden by directing both neutrophils and macrophages to damage larvae in the skin or lungs before they reach the gut.

Because neutrophils and IL-17 contribute to the lung damage associated with the migration of *N. brasiliensis* larvae[24], we assessed the lung condition of infected mice treated

with anti-Ym1. Such treatment blocked the influx of neutrophils into both the interstitial spaces and bronchoalveolar spaces, as well as the expression of genes encoding IL-17A and IL-17-driven chemokines in mice at day 2 after infection. As predicted by published work[24], this resulted in significantly less acute lung injury, an effect mirrored in mice deficient in IL-17A. Thus, Ym1 in the early innate stages of infection with *N. brasiliensis* promoted lung damage, presumably as a necessary consequence of limiting the number of parasites.

While the finding that a strongly T_H2-associated protein was able to drive the accumulation of neutrophils and contribute to injury responses may be somewhat unexpected, Ym1 has consistently been associated with acute injury[42,43], and indeed one of the first publications on Ym1 showed rapid Ym1 expression following a stab wound in the brain[44]. Such data, along with the ability of Ym1 and Ym2 to upregulate the expression of IL-1β and the number and activity of early responder $\gamma\delta$ T cells, indicate Ym1 and Ym2 are danger-associated molecular patterns (DAMPs) that form part of the innate immune response to trauma[45]. The possibility that CLPs act as DAMPs is supported by the finding that the induction of IL-17 and neutrophils was dependent on IL-1 signaling. Although Ym1 induced the release of IL-1 from peritoneal cells *in vitro*, the amount was far below that observed with well-known inflammasome activators (data not shown). We thus suspect that Ym1 was interacting with other components *in vivo* or was triggering the release of IL-1 from other sources, such as epithelial cells or platelets. CLPs are lectins that can bind heparan sulfate in the extracellular matrix and on the cell surface[46], and this might contribute to the release of IL-1 via receptor crosslinking or displacement of extracellular matrix–bound inflammasome mediators. Additionally, Ym1 has the propensity to form crystals in pathological conditions[47], which might directly activate the inflammasome *in vivo* but not under our *in vitro* conditions. These will be important avenues for further investigation, along with a specific assessment of the contributions of IL-1α versus IL-1β and the potential role of IL-18, as well as suppressed production of IFN-γ.

Despite its contribution to neutrophil mediated injury, a role for Ym1 in subsequent repair would be predicted from its very abundant production by IL-4-activated macrophages[48,49], and indeed this may be the case. At approximately day 4 after infection with *N. brasiliensis*, the immune response starts to switch to an adaptive one, with an increase in T_H2 cytokine expression[24,50], required for the expulsion of worms[51]. Repair of lung damage from

larval migration also requires a competent host adaptive response[52] and signaling via the receptor IL-4Rα[24] as well as an intact population of type 2 ILCs[53]. Notably, the chitin-driven γδ T cell response that has been reported was dampened by activated type 2 ILCs[19]. We saw no change in the number of ILCs in the short time frame of the infections with *N. brasiliensis*, but given that chitin is a structural component of many pathogens, including helminths, the ability to restrain excessive γδ T cell stimulation and the ensuing neutrophilic inflammation would be necessary for limiting damage to the host. Indeed, our data suggested that IL-17 itself would be able to promote the protective type 2 response, as IL-17A-deficient mice showed diminished type 2 cytokine responses and there appeared to be defects in lung repair at day 4. The idea that IL-17 can promote type 2 responses in the lung is not new and has been reported[54–56]. While our study has focused on the early innate events, further investigation would be needed to determine whether the Ym1-, Ym2- or even BRP-39-mediated IL-17A production contributes to later repair responses.

The chromosomal location of CLP-encoding genes suggests that mouse and human CLPs are derived from duplication and mutation of genes encoding the active chitinases[5]. Thus, despite the differences between species, CLPs as a family probably share common features. Elucidating why CLPs are undergoing such rapid divergence is an important challenge for understanding their function relative to their non-mutating enzymatically active relatives. Our studies have defined a previously unknown role for CLPs in innate immune defense against nematodes. In summary, we found that mouse CLPs promoted IL-17 responses and that Ym1 led to enhanced recruitment of neutrophils. The consequence of Ym1 function on infection with a nematode that migrates to the lungs was better control of the parasite but at the cost of increased acute lung damage.

METHODS

Methods and any associated references are available in the online version of the paper.

Note: Any Supplementary Information and Source Data files are available in the online version of the paper.

ACKNOWLEDGMENTS

AUTHOR CONTRIBUTIONS

COMPETING FINANCIAL INTERESTS

Figure 1 The expression of CLPs in mouse lungs. (**a**,**b**) Amplification of CLP-encoding mRNA in lung tissue from BALB/c mice treated with PBS or challenged with OVA (**a**) or BALB/c mice left uninfected (UI) or infected (inf) with *N. brasiliensis*, assessed at day 2 after infection (**b**), presented as SYBR green fluorescence versus cycle number (mRNA abundance); shaded areas indicate upregulation. (**c**) Microscopy of lung sections from PBS- or OVA-challenged mice, stained with anti-Ym1 or anti-BRP-39. Scale bar, 20 μm. Data are representative of three independent experiments (mean in **a**,**b**).

Figure 2 Overexpression of Ym1 in the lungs induces neutrophil accumulation. (**a**) Expression of CLP-encoding genes in total cells of BAL fluid obtained from BALB/c wild-type mice 48 h after intranasal transfection with 20 μg pcDNA3.1 or plasmid encoding BRP-39, Ym1 or Ym2, presented relative to results obtained with pcDNA3.1, set as 1 (10^0; gray horizontal line). (**b**,**c**) Absolute number of total cells in BAL fluid (**b**) and total cells per mg lung tissue (**c**) from mice as in **a**. (**d**) Absolute number of neutrophils in BAL fluid from mice treated as in **a**, assessed in cytospins stained with a modified Giemsa stain (**e**) Expression of the neutrophil marker Ly6G by single-cell suspensions of lung tissue from mice treated as in **a**. Numbers above outlined areas indicate percent Ly6G$^+$CD11b$^+$ neutrophils. Live/Dead (vertical axis), viability stain. (**f**) Absolute number of neutrophils in the lungs of mice as in **e**, normalized to lung weight. NS, not significant; *$P < 0.05$ and **$P < 0.0001$, compared with results obtained by transfection with pcDNA3.1 (analysis of variance (ANOVA) with the Tukey-Kramer honest significant difference

(HSD) multiple comparison test (**a**) or Kruskal-Wallis *post hoc* test (**b,d,f**)). Data were pooled from (**a–d,f**) or are representative of (**e**) two independent experiments with five to nine mice per group (mean and s.e.m. in **a–d,f**).

Figure 3 Ym1 promotes OVA-induced neutrophilia and regulates IL-17A abundance. (**a**) Total cells (left) and frequency of eosinophils (middle) and neutrophils (right) in BAL fluid from mice challenged with PBS or OVA (horizontal axis) and treated intraperitoneally with 200 μg IgG2a or anti-Ym1 (α-Ym1) (assessed as in **Fig. 2d**). (**b**) IL-17A in supernatants of thoracic lymph node cells obtained from mice challenged with PBS or OVA as in **a** and cultured with OVA antigen (Ag; 500 μg) or anti-CD3 (1 μg/ml), results are normalized to those obtained for splenocytes cultured with medium alone. (**c**) Expression of *Il17a* mRNA (left) and *Cxcl5* mRNA (right) in lung tissue from mice as in **a**; results are presented relative to those of the housekeeping gene *Rpl13a* (encoding ribosomal protein L13A). ND, not detected. *$P < 0.05$, **$P < 0.01$, ***$P < 0.001$ and ****$P < 0.0001$, compared with results obtained with PBS and IgG2a or OVA and IgG2a (ANOVA with the Tukey-Kramer HSD multiple-comparison test (**a,c**) or the Kruskal-Wallis test (**b**)). Data were pooled from (**a**) or are representative of (**b,c**) two independent experiments with eleven to twelve mice per group (mean and s.e.m.).

Figure 4 CLPs alter the recruitment of neutrophils into the peritoneal cavity. (**a**) Expression of CLP-encoding genes in PECs collected at 48 h from BALB/c wild-type mice treated intraperitoneally with pcDNA3.1 or plasmid encoding BRP-39, Ym1 or Ym2 (20 μg) or glucose (presented as in **Fig. 2a**). (**b**) Absolute number of viable cells (left) and Ly6G$^+$Cd11b$^+$F4/80$^-$ neutrophils (right) among PECs from mice as in **a**. (**c**) *Il17a* expression in PECs from mice as in **a** (presented as in **Fig. 3c**). (**d**) Expression of IL-17A in PECs obtained from mice as in **a** and stimulated *ex vivo* with PMA and ionomycin. (**e**) Absolute number of IL-17$^-$ or IL-17$^+$ cells expressing the γδ T cell antigen receptor (TCRγδ$^+$), from mice as in **a**. Asterisks above the bars indicate the significance of results obtained for IL-17$^+$ TCRγδ$^+$ cells and asterisks (and NS) inside the bars indicate significance of results obtained for total TCRγδ$^+$ cells. (**f,g**) Expression of *Il1b* mRNA (**f**) and *Il18* mRNA (**g**) in PECs from mice as in **a** (presented as in **Fig. 3c**). (**h**) Expression of IL-17A in PECs collected from mice 48 h after intraperitoneal transfection of pcDNA3.1 or plasmid encoding Ym1 and intraperitoneal treatment with PBS or anakinra (Ank; 100 mg per kg body weight), and then stimulated *in vitro* with PMA and ionomycin. (**i**) Absolute number of neutrophils among PECs from mice as in **h** (analyzed as in **b**). *$P < 0.05$, **$P < 0.01$, ***$P < 0.001$

and ****$P < 0.0001$, compared with results obtained by transfection of pcDNA3.1 (ANOVA with
the Tukey-Kramer HSD multiple-comparison test). Data were pooled from two independent
experiments with eight to eleven mice per group (**a–c,e–g**; mean and s.e.m.) or are
representative of two independent experiments with five to seven mice per group (**d,h,i**; mean
and s.e.m. in **i**).

Figure 5 Ym1-induced recruitment of neutrophils contributes to acute lung injury following
infection with *N. brasiliensis*. (**a**) Absolute number of neutrophils (top) and macrophages
(bottom) in BAL fluid from BALB/c wild-type mice left uninfected or infected with 500 *N.
brasiliensis* larvae (L3) (day 0) and treated intraperitoneally with anti-Ym1 or IgG2a (days –1 to
+1), harvested at day 2 or 4 after infection (assessed as in **Fig. 2d**). (**b**) Absolute number of
Ly6G$^+$Cd11b$^+$F4/80$^-$ neutrophils (top) and F4/80$^+$Cd11b$^+$CD11c$^-$ interstitial macrophages
(bottom) in lung tissue from mice as in **a**. (**c–e**) Expression of *Il17a* mRNA (**c**), *Cxcl5* mRNA (**d**)
and *Il1b* mRNA (**e**) in lungs of mice as in **a** (presented as in **Fig. 3c**). (**f**) IL-1β in lung
homogenates from mice as in **a** (per mg total lung protein). (**g**) Microscopy of lung sections
from mice as in **a**, stained with hematoxylin and eosin (top), and quantification of lung damage,
calculated as 'linear means intercept' (below). Scale bars, 200 μm. *$P < 0.05$, **$P < 0.01$, ***$P <
0.001$ and ****$P < 0.0001$, compared with results obtained for treatment with IgG2a or results
at day 2 (ANOVA with the Tukey-Kramer HSD multiple-comparison test). Data are
representative from three independent experiments (mean and s.e.m. of six mice per group).

Figure 6 IL-17A production by γδ T cells contributes to *N. brasiliensis*–mediated lung injury. (**a**)
Absolute number of neutrophils in BAL fluid from C57BL/6 wild-type mice (WT) or
Il17a^{Cre}*Rosa26*^{eYFP} mice (IL-17A-KO) left uninfected or infected with 500 *N. brasiliensis* larvae
(L3), harvested at day 2 or 4 after infection (assessed as in **Fig. 2d**). (**b**) Microscopy of lung
sections from mice as in **a**, stained with hematoxylin and eosin (left), and lung damage in mice
as in **a** (right) (calculated as in **Fig. 5g**). Scale bars (left), 200 μm. (**c**) IL-13 in supernatants of
splenocytes obtained from mice as in **a** and cultured with *N. brasiliensis* excretory secretory
antigen (Ag; 1 μg/ml) or anti-CD3 (1 μg/ml); results are normalized to those obtained for
splenocytes cultured with medium alone. (**d**) Expression of IL-17A in single-cell suspensions of
lung tissue from C57BL/6 wild-type mice as in **a**, stimulated *ex vivo* with PMA and ionomycin.
(**e**) Absolute number of IL-17A$^-$ or IL-17A$^+$ TCRγδ$^+$ cells from mice as in **a**. Asterisks above the
bars indicate the significance of results obtained for IL-17$^+$ TCRγδ$^+$ cells and asterisks inside the

bars indicate significance of results obtained for total TCRγδ$^+$ cells. *$P < 0.05$, **$P < 0.01$, ***$P < 0.001$ and ****$P < 0.0001$, compared with uninfected wild-type mice or wild-type mice at day 2 or day 4 after infection (ANOVA with the Kruskal-Wallis test (**a**) or the Tukey-Kramer HSD multiple-comparison test (**b–e**)). Data were pooled from (**a–c,e**) or are representative of (**d**) two independent experiments with five to twelve mice per group (mean and s.e.m. in **a–c,e**).

Figure 7 BRP-39 regulates IL-17A production in γδ T cells in the lungs. (**a**) *Il17a* expression in lungs of C57BL/6 wild-type mice (WT) or *Chil1*$^{−/−}$ mice (BRP-39-KO) left uninfected or infected with 500 *N. brasiliensis* larvae (L3), assessed at day 2 or 4 after infection (presented as in **Fig. 3c**). (**b**) Absolute number of IL-17$^−$ or IL-17$^+$ γδ T cells in lungs of mice as in **a**. Asterisks (and NS) above the bars indicate the significance of results obtained for IL-17$^+$ TCRγδ$^+$ cells and asterisks (and dagger) inside the bars indicate significance of results obtained for total TCRγδ$^+$ cells. (**c**) Absolute number of Ly6G$^+$CD11b$^+$F4/80$^−$ neutrophils in lung tissue of mice as in **a**. (**d**) Expression of *Il1b* mRNA, *Il23p19* mRNA and *Il18* mRNA in lungs of mice as in **a** (presented as in **Fig. 3c**). *$P < 0.05$, **$P < 0.01$ and ***$P < 0.001$, compared with uninfected wild-type mice or wild-type mice on day 2 or day 4 after infection (**a–c**), †$P < 0.01$, compared with wild-type mice on day 4 infection (**b**) (ANOVA with the Tukey-Kramer HSD multiple-comparison test). Data are representative of two independent experiments with twelve to six mice per group (mean and s.e.m.).

Figure 8 IL-17A and Ym1 limit worm burden. (**a**-**c**) Expression of actin-encoding mRNA by *N. brasiliensis* (*Nb-ad1* mRNA) in whole lung tissue from BALB/c wild-type mice treated intraperitoneally with anti-Ym1 or IgG2a (on days −1 to +1 relative to infection at day 0) (**a**), C57BL/6 or *Il17a*^{Cre}*Rosa26*^{eYFP} mice (**b**) or C57BL/6 (wild-type) or *Chil1*$^{−/−}$ mice (**c**), all left uninfected or infected with 500 *N. brasiliensis* larvae (L3) and assessed at day 2 or 4 after infection. (**d–f**) Larvae in the small intestine (at day 4) in BALB/c mice as in **a** (**d**), C57BL/6 or *Il17a*^{Cre}*Rosa26*^{eYFP} mice as in **b** (**e**) or C57BL/6 or *Chil1*$^{−/−}$ mice as in **c** (**f**). (**g**) Microscopy of lung sections from mice at day 2 after infection as in **a** (top), and sections from mice treated with IgG2a as in **a** (bottom), stained with antibody to myeloperoxidase (MPO) and with the DNA-binding dye DAPI: white arrowheads, neutrophils; dotted line, *N. brasiliensis* larvae. Scale bars, 50 μm (top) or 100 μm (bottom). (**h–j**) Neutrophil swarms per section (**h**), neutrophils per swarm (**i**) and distribution frequency of neutrophils in swarms (**j**) in lung sections from mice as in **g**. Each symbol (**i**) represents one swarm. (**k,l**) Larvae (at day 4) in the small intestine (**k**) and

sections of the intestine (**l**) of BALB/c wild-type mice transfected intranasally with pcDNA3.1 or plasmid encoding Ym1 and infected with 500 *N. brasiliensis* larvae (L3). *$P < 0.05$, **$P < 0.01$, ***$P < 0.001$ and ****$P < 0.0001$ (ANOVA with the Tukey-Kramer HSD multiple-comparison test (**a–c,i**), unpaired *t*-test (**d–f**) or Wilcoxin nonparametric *t*-test (**h,i**)). Data are representative of two independent experiments with six to eight (**a–f**) or nine (**k,l**) mice per group (**a–f,k,l**; mean and s.e.m.) or one experiment with three mice per group (**g–j**; mean and s.e.m. in **h–j**).

Table 1 CLP-encoding mRNA in mouse lungs

AAI model	PBS challenge	OVA challenge
Chil1	0.88 ± 0.40	2.32 ± 0.50*
Chil3	1.06 ± 0.33	18.48 ± 2.83***
Chil4	0.20 ± 0.15	309.97 ± 11.53*

N. brasiliensis model	Uninfected	Day 2 after infection
Chil1	1.03 ± 0.12	1.85 ± 0.33
Chil3	1.03 ± 0.14	1.97 ± 0.27*
Chil4	5.93 ± 2.91	10634 ± 7227**

Expression of CLP-encoding mRNA in lungs of mice treated to induce allergic airway inflammation (AAI) and challenged with PBS or OVA (top) or mice left uninfected or assessed 2 d after infection with *N. brasiliensis* (bottom). *$P < 0.05$, **$P < 0.01$ and ***$P < 0.001$, compared with PBS challenge or no infection (Student's *t*-test). Data are from three independent experiments with of six mice (PBS) or nine mice (OVA) (mean ± s.e.m.).

ONLINE METHODS

Mice. Wild-type (BALB/c or C57BL/6) mice, *Rag2*$^{-/-}$ (BALB/c) mice, *Chil1*$^{-/-}$ (C57BL/6) mice[9] and C57BL/6 *Il17a*^{Cre}*Rosa26*^{eYFP} mice[25] were bred at the University of Edinburgh. Mice were 7–12-weeks old at the start of the experiment, and all mice were housed in individually ventilated cages. Mice were not randomized in cages, but each cage was randomly assigned to a treatment group. Investigators were not blinded to mouse identity during necropsy. Experiments were in accordance with the United Kingdom Animals (Scientific Procedures) Act of 1986. All experiments used female mice, except for experiments with wild-type mice and *Il17a*^{Cre}*Rosa26*^{eYFP} mice and anakinra experiments (**Figs. 4** and **6**), which used mice of both sexes. Sample size was calculated on the basis of the number of animals needed for detection

of a change in neutrophil numbers of 25% at a *P* value of <0.05, based on published experiments[13].

Anti-Ym1. The anti-Ym1 mouse hybridoma cell line 4D10 was generated by immunization of mice with a Ym1 peptide (sequence, IPRLLLTSTGAGIID) conjugated to keyhole limpet hemocyanin and has been shown to be neutralizing[14]. The neutralizing activity of the monoclonal antibody was verified *in vitro*. The hybridoma cell line 2D12 from the European Collection of Cell Cultures was used as the IgG2a isotype-matched control antibody. Secreted antibodies were purified by protein G affinity chromatography.

Plasmids. The full-length coding regions of mouse *Chil1*, *Chil3* and *Chil4* were amplified with a mouse lung cDNA template. The cDNA fragments were directionally cloned into pcDNA3.1 (Invitrogen) to generate plasmids encoding V5- and histidine-tagged CLPs. TOP10 competent cells were transformed with CLP-encoding plasmid or pcDNA3.1 and sequences were confirmed. Plasmids were routinely grown in transformed JM109 competent cells (Promega) and plasmids were isolated with miniprep kits (Qiagen) before undergoing removal of endotoxin (MiraCLEAN Kit; Mirus) and concentration of plasmid. The DNA concentration was quantified by fluorometric methods (Qubit; Life Technologies).

***In vivo* transfection.** The plasmid pcDNA3.1 (control) or plasmid encoding BRP-39, Ym1 or Ym2 were made into complexes with *in vivo* JetPEI (Polyplus Transfection) at an 'N:P' ratio of 8 (number of nitrogen residues of jetPEI per DNA phosphate). Complexes were administered to mice at a dose 20 μg of plasmid via an intranasal or intraperitoneal route. Either BAL fluid and lungs or PECs were harvested 48 h after transfection. Mice that were not transfected were excluded from the analysis.

Blockade of the IL-1 receptor. BALB/c wild-type mice received two intraperitoneal doses of or PBS (vehicle) or anakinra; recombinant methionyl human IL-1 receptor antagonist (Kineret; Amgen) at a dose of 100 mg per kg body weight at 4 and 24 h after transfection of pcDNA3.1 or plasmid encoding Ym1 (20 μg, given intraperitoneally).

Allergic inflammation. Allergic airway inflammation was induced in mice in a manner similar to one that has been described[13]. BALB/c mice were sensitized (on day 0) with 20 μg OVA precipitated with alum, administered intraperitoneally before 30 min aerosol challenges with PBS or 1% OVA on days 8, 9 and 10 (Supplementary Fig. 2). Mice were treated intraperitoneally

with 200 μg anti-Ym1 or IgG2a 1 d before challenge and every day thereafter. On day 11, BAL
was performed and lungs were taken for further assays and analysis.

***N. brasiliensis* infection.** *N. brasiliensis* was maintained by serial passage through Sprague-
Dawley rats, as described[57]. Third-stage larvae (larvae at L3) were washed ten times with sterile
PBS before infection. On day 0, BALB/c wild-type mice were infected subcutaneously with 500
larvae (L3), then were treated intraperitoneally with 200 μg anti-Ym1 or IgG2a on days –1, 0
and 1 (relative to infection on day 0). Additionally, C57BL/6 wild-type mice, *Chil1*$^{-/-}$ (C57BL/6)
mice or *Il17a*^{Cre}*Rosa26*^{eYFP} mice were infected subcutaneously d with 500 *N. brasiliensis* larvae
(L3) on day 0. On days 2 and 4, BAL was performed and lungs were taken for further assays and
analysis. Single-cell suspensions of splenocytes were stimulated *ex vivo* with *N. brasiliensis*
excretory secretory product antigen[58] (1 μg/ml) or anti-CD3 (1 μg/ml). Cell supernatants were
harvested 72 h later and were stored at –20 °C until further analysis. BALB/c wild-type mice
were also given pcDNA3.1 or plasmid encoding Ym1 (20μg) intranasally 1 d before
subcutaneous infection with 500 *N. brasiliensis* larvae (L3). On day 4 after infection, the small
intestines of infected mice were collected in Dulbecco's-PBS (Sigma) and worms therein were
counted.

Histology and immunofluorescence. Cytospins were prepared from cells in BAL fluid and were
stained with Kwik-Diff (Thermo Scientific). Lung tissue was fixed perfused with 10% neutral
buffered formalin (Sigma) and was incubated overnight before being transferred to 70%
ethanol. Lungs were embedded in paraffin, then were cut into sections and stained with
hematoxylin and eosin. The 'linear means intercept' method was used for quantification of
emphysema-like damage[59]. For calculation of the 'linear means intercept', lung samples were
stained with hematoxylin and eosin and then were viewed by microcopy with an original
magnification of ×200; 15 random nonoverlapping fields per sample were assessed. Six
horizontal lines were drawn across each image (ImageJ software, version 1.44) and the total
alveolar wall intercepts per line were counted. The length of each line was then divided by the
number of intercepts to calculate the 'linear means intercept' value. Images that included large
bronchi and vessels were avoided, and randomly assigned samples were analyzed by
researchers 'blinded' to sample identity. For immunofluorescence imaging, lung sections were
deparaffinized and then were incubated for 45 min at 97 °C in Target Retrieval Solution, pH 9.0
(S2368; Dako) for antigen retrieval and were stained with rabbit polyclonal antibody to

myeloperoxidase (1:200 in 2% BSA, 2% donkey serum; GA511; Dako) and with DAPI (4,6-diamidino-2-phenylindole) for staining of DNA, for study of patterns of neutrophil recruitment. Swarms were identified by analysis of myeloperoxidase-labeled images with ImageJ software. A binary image was created with the threshold function to mark individual cells, then a Voronoi binary analysis was applied and subsequently inverted. That image was then analyzed by the filtering out of large Voronoi tiles through the use of upper area limits to create a mask with regions of interest that covered lung areas containing closely clustered neutrophils. Adjacent tiles were clustered into a single swarm. Those masks were also applied to the original images of individual cells to obtain the number of neutrophils in each cluster.

Extraction of RNA and quantitative real-time PCR. A section of the right lung lobe was stored in RNAlater (Ambion) before homogenization of tissue in Trifast GOLD (Peqlab) with a TissueLyser (Qiagen), and RNA was prepared according to the Trifast manufacturer's instructions. For reverse transcription, 0.25–1.00 μg of total RNA was treated with 50 U Tetro reverse transcriptase (Bioline), 40 mM dNTPs (Promega), 0.5 μg primer for cDNA synthesis (Roche) and RNasin inhibitor (Promega). The abundance of transcripts from the genes of interest was measured by real-time PCR with the Lightcycler 480 II system (Roche) with a SYBR Green I Master kit (Roche) and specific primer pairs (**Supplementary Table 1**) as described[13]. PCR amplification was analyzed by the second-derivative maximum algorithm (LightCycler 480 Sw 1.5; Roche), and expression of the gene of interest was normalized to that of the housekeeping gene *Rpl13a*.

Flow cytometry. Single-cell suspensions of the right lung lobe were prepared by digestion for 25 min at 37 °C with 0.2 U/ml Liberase TL (Roche) and 80 U/ml DNase (Life Tech) in Hank's balanced-salt solution, followed by forcing of tissue suspensions through gauze. Red blood cells were lysed (Sigma) and then total cells were counted with a Scharf Instruments cell counter (Roche) or an automated Cellometer T4 (Peqlab). Cells were incubated with Fc block (CD16/CD32 and mouse serum) and were stained with fluorescence-conjugated anti-CD11b (M1/70), anti-CD11c (N418), anti-F4/80 (BM8), anti-Ly6G (1A8), anti-CD4 (GK1.5), anti-CD8 (52-6.7), anti-TCRγδ (GL3), anti-CD90.2 (30-H12), anti-CD25 (PC61) and anti-CD127 (A7R34; all from Biolegend); and antibody to I-A–I-E (major histocompatibility complex class II; M5/114.15.2), anti-CD19 (6D5) and anti-TCRβ (H57-597; all from eBioscience); and anti–Siglec F (E50-2440; BD Biosciences). Cells were identified by expression of surface markers as follows: neutrophils

were CD11b$^+$Ly6G$^+$F4/80$^-$; interstitial lung macrophages were F4/80$^+$CD11b$^+$CD11c$^-$Siglec F$^-$; $\gamma\delta$ T cells were TCR$\gamma\delta^+$TCRβ^-CD4$^-$CD8$^-$CD11b$^-$; and ILCs were negative for lineage markers (CD3, CD19, F4/80, SigF, Ly6G, CD11c, CD11b and Ter119) and were CD90.2$^+$CD25$^+$CD127$^+$. Cells were fixed for 10 min at 20 °C with 2% paraformaldehyde and were stored at 4 °C until intracellular staining or acquisition. For staining of intracellular IL-17A, cells were stimulated for 4 h at 37 °C with PMA (phorbol myristate acetate; 0.5 μg/ml) and ionomycin (1 μg/ml) and for 3 h at 37 °C with brefaldin A (10 μg/ml; Sigma). Cell surfaces were stained (antibodies identified above) and then cells were fixed with 2% paraformaldehyde and then permeabilized according to the manufacturer's instructions (eBioscience), then were stained with allophycocyanin-conjugated antibody to mouse IL-17A (TC11-18H10.1; Biolegend) or allophycocyanin-conjugated antibody to mouse IgG1 (isotype-matched control antibody; MOPC-21; Biolegend) and Alexa Fluor 488–conjugated antibody to mouse IFN-γ (XMG1.2; Biolegend) or Alexa Fluor 488–conjugated antibody to mouse IgG1 (i isotype-matched control antibody; MOPC-21; Biolegend), before acquisition. Live/Dead Aqua (Life Technologies) was used for exclusion of dead cells from analysis. Samples were analyzed by flow cytometry with a FACSCanto II or LSR II (Becton-Dickinson) and cells were characterized with FlowJo software.

Quantification of cytokines. A Mouse IL-17 and IL-13 DuoSet ELISA kit (R&D Systems) was used for measurement of IL-17A and IL-13 in thoracic lymph node or splenocyte culture supernatants following stimulation for 72 h with OVA or *N. brasiliensis* excretory secretory antigen or anti-CD3 mitogen. Whole lung tissue was homogenized in Hank's balanced-salt solution containing protease inhibitor 'cocktail' (Sigma). The concentration of IL-1β protein was measured in homogenate supernatant by enzyme-linked immunosorbent assay (eBioscience).

Statistical analysis. JMP software (JMP 11; SAS Institute) was used for statistical analysis. Normal distribution of data was determined by visual examination of residuals, and each group was tested for unequal variance by Welch's test. Differences between groups were assessed by ANOVA followed by the Tukey-Kramer HSD multiple-comparison test or unpaired two-tailed Student's *t*-test. In some cases, data were log-transformed to achieve normal distribution. However, in situations in which this was not possible, the Kruskal-Wallis test was used. Differences with a *P* value of less than 0.05 were considered statistically significant.

References

1.   Sutherland, T.E., Maizels, R.M. & Allen, J.E. Chitinases and chitinase-like proteins: potential therapeutic targets for the treatment of T-helper type 2 allergies. *Clin. Exp. Allergy* **39,** 943-955 (2009).

2.   Labadaridis, I. *et al.* Chitotriosidase in neonates with fungal and bacterial infections. *Arch. Dis. Child Fetal Neonatal Ed.* **90,** F531-532 (2005).

3.   Barone, R. *et al.* Plasma chitotriosidase activity in acute Plasmodium falciparum malaria. *Clin. Chim. Acta* **331,** 79-85 (2003).

4.   Nance, J.P. *et al.* Chitinase dependent control of protozoan cyst burden in the brain. *PLoS Pathog.* **8,** e1002990 (2012).

5.   Bussink, A.P., Speijer, D., Aerts, J.M. & Boot, R.G. Evolution of mammalian chitinase(-like) members of family 18 glycosyl hydrolases. *Genetics* **177,** 959-970 (2007).

6.   Lee, C.G. *et al.* Role of chitin and chitinase/chitinase-like proteins in inflammation, tissue remodeling, and injury. *Annu. Rev. Physiol.* **73,** 479-501 (2011).

7.   Webb, D.C., McKenzie, A.N. & Foster, P.S. Expression of the Ym2 lectin-binding protein is dependent on interleukin (IL)-4 and IL-13 signal transduction: identification of a novel allergy-associated protein. *J Biol Chem* **276,** 41969-41976 (2001).

8.   Welch, J.S. *et al.* TH2 cytokines and allergic challenge induce Ym1 expression in macrophages by a STAT6-dependent mechanism. *J Biol Chem* **277,** 42821-42829 (2002).

9.   Lee, C.G. *et al.* Role of breast regression protein 39 (BRP-39)/chitinase 3-like-1 in Th2 and IL-13-induced tissue responses and apoptosis. *J. Exp. Med.* **206,** 1149-1166 (2009).

10.   Sohn, M.H. *et al.* The chitinase-like proteins breast regression protein-39 and YKL-40 regulate hyperoxia-induced acute lung injury. *Am. J. Respir. Crit. Care. Med.* **182,** 918-928 (2010).

11. Hector, A. *et al.* The chitinase-like protein YKL-40 modulates cystic fibrosis lung disease. *PLoS One* **6,** e24399 (2011).

12. Nikota, J.K. *et al.* Differential expression and function of breast regression protein 39 (BRP-39) in murine models of subacute cigarette smoke exposure and allergic airway inflammation. *Respir. Res.* **12,** 39 (2011).

13. Sutherland, T.E. *et al.* Analyzing airway inflammation with chemical biology: dissection of acidic mammalian chitinase function with a selective drug-like inhibitor. *Chem. Biol.* **18,** 569-579 (2011).

14. Arora, M. *et al.* Simvastatin promotes Th2-type responses through the induction of the chitinase family member Ym1 in dendritic cells. *Proc. Natl. Acad. Sci. U S A* **103,** 7777-7782 (2006).

15. Ye, P. *et al.* Requirement of interleukin 17 receptor signaling for lung CXC chemokine and granulocyte colony-stimulating factor expression, neutrophil recruitment, and host defense. *J. Exp. Med.* **194,** 519-527 (2001).

16. Aujla, S.J. & Alcorn, J.F. T(H)17 cells in asthma and inflammation. *Biochim. Biophys. Acta* **1810,** 1066-1079 (2011).

17. Raz, E. Organ-specific regulation of innate immunity. *Nat. Immunol.* **8,** 3-4 (2007).

18. Lalor, S.J. *et al.* Caspase-1-processed cytokines IL-1beta and IL-18 promote IL-17 production by gammadelta and CD4 T cells that mediate autoimmunity. *J. Immunol.* **186,** 5738-5748 (2011).

19. Van Dyken, S.J. *et al.* Chitin Activates Parallel Immune Modules that Direct Distinct Inflammatory Responses via Innate Lymphoid Type 2 and gammadelta T Cells. *Immunity* **40,** 414-424 (2014).

20. Nielsen, M.M. *et al.* IL-1beta-dependent activation of dendritic epidermal T cells in contact hypersensitivity. *J. Immunol.* **192,** 2975-2983 (2014).

21. Osborne, L.C. *et al.* Coinfection. Virus-helminth coinfection reveals a microbiota-independent mechanism of immunomodulation. *Science* **345,** 578-582 (2014).

22. Gladiator, A., Wangler, N., Trautwein-Weidner, K. & LeibundGut-Landmann, S. Cutting edge: IL-17-secreting innate lymphoid cells are essential for host defense against fungal infection. *J. Immunol.* **190,** 521-525 (2013).

23. Kim, H.Y. *et al.* Interleukin-17-producing innate lymphoid cells and the NLRP3 inflammasome facilitate obesity-associated airway hyperreactivity. *Nat. Med.* **20,** 54-61 (2014).

24. Chen, F. *et al.* An essential role for TH2-type responses in limiting acute tissue damage during experimental helminth infection. *Nat. Med.* **18,** 260-266 (2012).

25. Hirota, K. *et al.* Fate mapping of IL-17-producing T cells in inflammatory responses. *Nat. Immunol.* **12,** 255-263 (2011).

26. Li, C. *et al.* IL-17 response mediates acute lung injury induced by the 2009 pandemic influenza A (H1N1) virus. *Cell Res.* **22,** 528-538 (2012).

27. Grommes, J. & Soehnlein, O. Contribution of neutrophils to acute lung injury. *Mol. Med.* **17,** 293-307 (2011).

28. The ENFUMOSA cross-sectional European multicentre study of the clinical phenotype of chronic severe asthma. European Network for Understanding Mechanisms of Severe Asthma. *Eur. Respir. J.* **22,** 470-477 (2003).

29. Al-Ramli, W. *et al.* T(H)17-associated cytokines (IL-17A and IL-17F) in severe asthma. *J. Allergy Clin. Immunol.* **123,** 1185-1187 (2009).

30. Newcomb, D.C. & Peebles, R.S., Jr. Th17-mediated inflammation in asthma. *Curr. Opin. Immunol.* **25,** 755-760 (2013).

31. Letuve, S. *et al.* YKL-40 is elevated in patients with chronic obstructive pulmonary disease and activates alveolar macrophages. *J. Immunol.* **181,** 5167-5173 (2008).

32. Vind, I., Johansen, J.S., Price, P.A. & Munkholm, P. Serum YKL-40, a potential new marker of disease activity in patients with inflammatory bowel disease. *Scand. J. Gastroenterol.* **38,** 599-605 (2003).

33. Alcorn, J.F., Crowe, C.R. & Kolls, J.K. TH17 cells in asthma and COPD. *Annu. Rev. Physiol.* **72,** 495-516 (2010).

34. Morrison, P.J., Ballantyne, S.J. & Kullberg, M.C. Interleukin-23 and T helper 17-type responses in intestinal inflammation: from cytokines to T-cell plasticity. *Immunology* **133,** 397-408 (2011).

35. Konradsen, J.R. *et al.* The chitinase-like protein YKL-40: A possible biomarker of inflammation and airway remodeling in severe pediatric asthma. *J. Allergy Clin. Immunol.* (2013).

36. Dela Cruz, C.S. *et al.* Chitinase 3-like-1 promotes Streptococcus pneumoniae killing and augments host tolerance to lung antibacterial responses. *Cell Host Microbe* **12,** 34-46 (2012).

37. Sakazaki, Y. *et al.* Overexpression of chitinase 3-like 1/YKL-40 in lung-specific IL-18-transgenic mice, smokers and COPD. *PLoS One* **6,** e24177 (2011).

38. Tran, H.T., Barnich, N. & Mizoguchi, E. Potential role of chitinases and chitin-binding proteins in host-microbial interactions during the development of intestinal inflammation. *Histol. Histopathol.* **26,** 1453-1464 (2011).

39. Anthony, R.M. *et al.* Protective immune mechanisms in helminth infection. *Nat. Rev. Immunol.* **7,** 975-987 (2007).

40. Bonne-Annee, S. *et al.* Human and mouse macrophages collaborate with neutrophils to kill larval Strongyloides stercoralis. *Infect. Immun.* **81,** 3346-3355 (2013).

41. O'Connell, A.E. *et al.* Major basic protein from eosinophils and myeloperoxidase from neutrophils are required for protective immunity to Strongyloides stercoralis in mice. *Infect. Immun.* **79,** 2770-2778 (2011).

42. Loke, P. *et al.* Alternative activation is an innate response to injury that requires CD4+ T cells to be sustained during chronic infection. *J. Immunol.* **179,** 3926-3936 (2007).

43. Ydens, E. *et al.* Acute injury in the peripheral nervous system triggers an alternative macrophage response. *J. Neuroinflammation* **9,** 176 (2012).

44.   Hung, S.I., Chang, A.C., Kato, I. & Chang, N.C. Transient expression of Ym1, a heparin-binding lectin, during developmental hematopoiesis and inflammation. *J. Leukoc. Biol.* **72,** 72-82 (2002).

45.   Pittman, K. & Kubes, P. Damage-associated molecular patterns control neutrophil recruitment. *J. Innate. Immun.* **5,** 315-323 (2013).

46.   Prakash, M. *et al.* Diverse pathological implications of YKL-40: answers may lie in 'outside-in' signaling. *Cellular signalling* **25,** 1567-1573 (2013).

47.   Guo, L., Johnson, R.S. & Schuh, J.C. Biochemical characterization of endogenously formed eosinophilic crystals in the lungs of mice. *J Biol Chem* **275,** 8032-8037 (2000).

48.   Falcone, F.H. *et al.* A Brugia malayi homolog of macrophage migration inhibitory factor reveals an important link between macrophages and eosinophil recruitment during nematode infection. *J. Immunol.* **167,** 5348-5354 (2001).

49.   Loke, P. *et al.* IL-4 dependent alternatively-activated macrophages have a distinctive in vivo gene expression phenotype. *BMC Immunol.* **3,** 7 (2002).

50.   Voehringer, D., Shinkai, K. & Locksley, R.M. Type 2 immunity reflects orchestrated recruitment of cells committed to IL-4 production. *Immunity* **20,** 267-277 (2004).

51.   Urban, J.F., Jr. *et al.* IL-13, IL-4Ralpha, and Stat6 are required for the expulsion of the gastrointestinal nematode parasite Nippostrongylus brasiliensis. *Immunity* **8,** 255-264 (1998).

52.   Reece, J.J., Siracusa, M.C. & Scott, A.L. Innate immune responses to lung-stage helminth infection induce alternatively activated alveolar macrophages. *Infect. Immun.* **74,** 4970-4981 (2006).

53.   Turner, J.E. *et al.* IL-9-mediated survival of type 2 innate lymphoid cells promotes damage control in helminth-induced lung inflammation. *J. Exp. Med.* **210,** 2951-2965 (2013).

54.   Kallal, L.E. *et al.* Inefficient lymph node sensitization during respiratory viral infection promotes IL-17-mediated lung pathology. *J. Immunol.* **185,** 4137-4147 (2010).

55.   Lajoie, S. *et al.* Complement-mediated regulation of the IL-17A axis is a central genetic determinant of the severity of experimental allergic asthma. *Nat. Immunol.* **11,** 928-935 (2010).

56.   Wang, M. *et al.* Immunomodulatory effects of IL-23 and IL-17 in a mouse model of allergic rhinitis. *Clin. Exp. Allergy* **43,** 956-966 (2013).

57.   Lawrence, R.A., Gray, C.A., Osborne, J. & Maizels, R.M. Nippostrongylus brasiliensis: cytokine responses and nematode expulsion in normal and IL-4-deficient mice. *Exp. Parasitol.* **84,** 65-73 (1996).

58.   Holland, M.J., Harcus, Y.M., Riches, P.L. & Maizels, R.M. Proteins secreted by the parasitic nematode Nippostrongylus brasiliensis act as adjuvants for Th2 responses. *Eur. J. Immunol.* **30,** 1977-1987 (2000).

59.   Thurlbeck, W.M. Measurement of pulmonary emphysema. *The American review of respiratory disease* **95,** 752-764 (1967).

a

b

c Ym1 BRP-39

Chil1 PBS — *Chil1* OVA
Chil3 PBS — *Chil3* OVA
Chil4 PBS — *Chil4* OVA

Chil1 naive — *Chil1* infected
Chil3 naive — *Chil3* infected
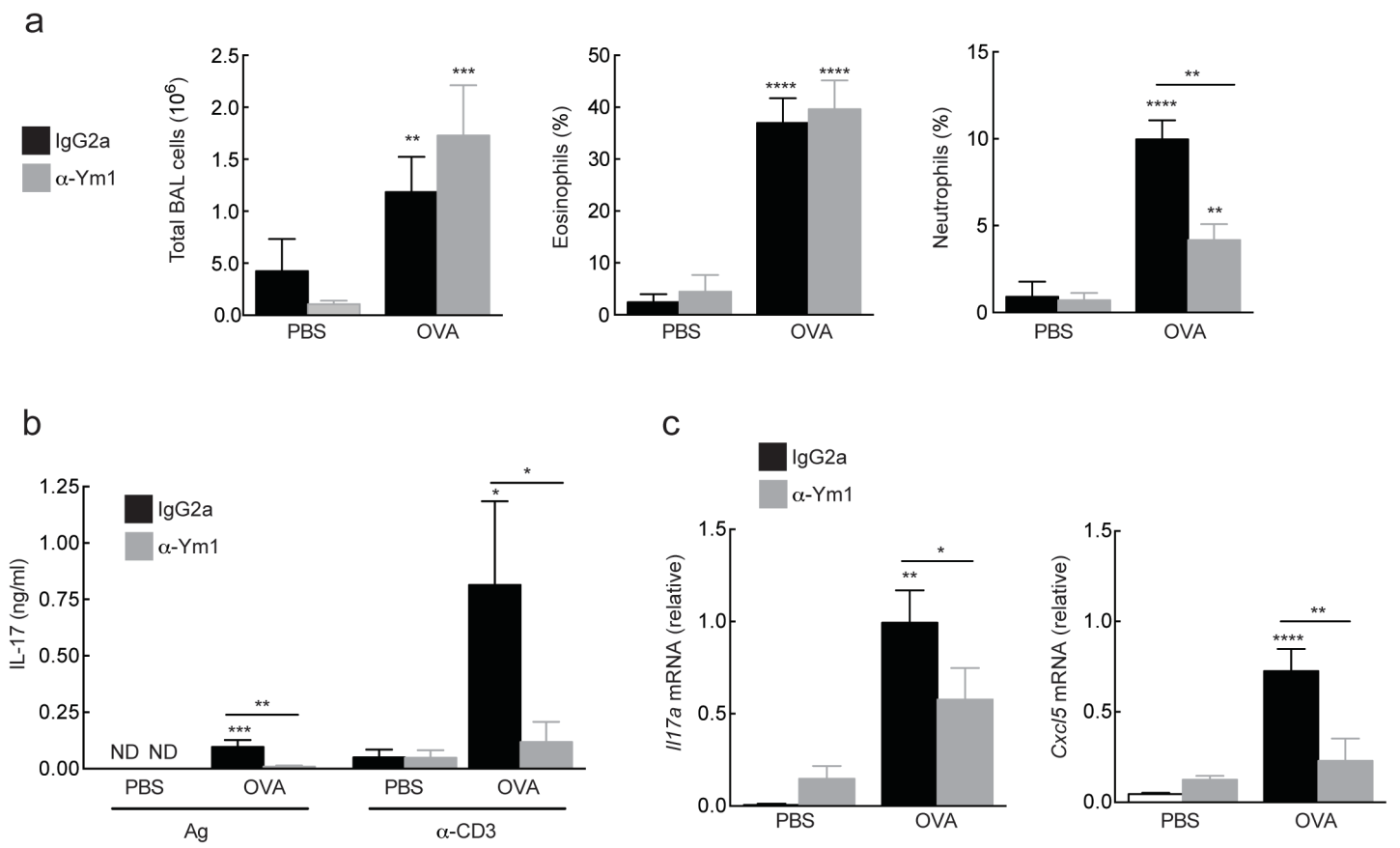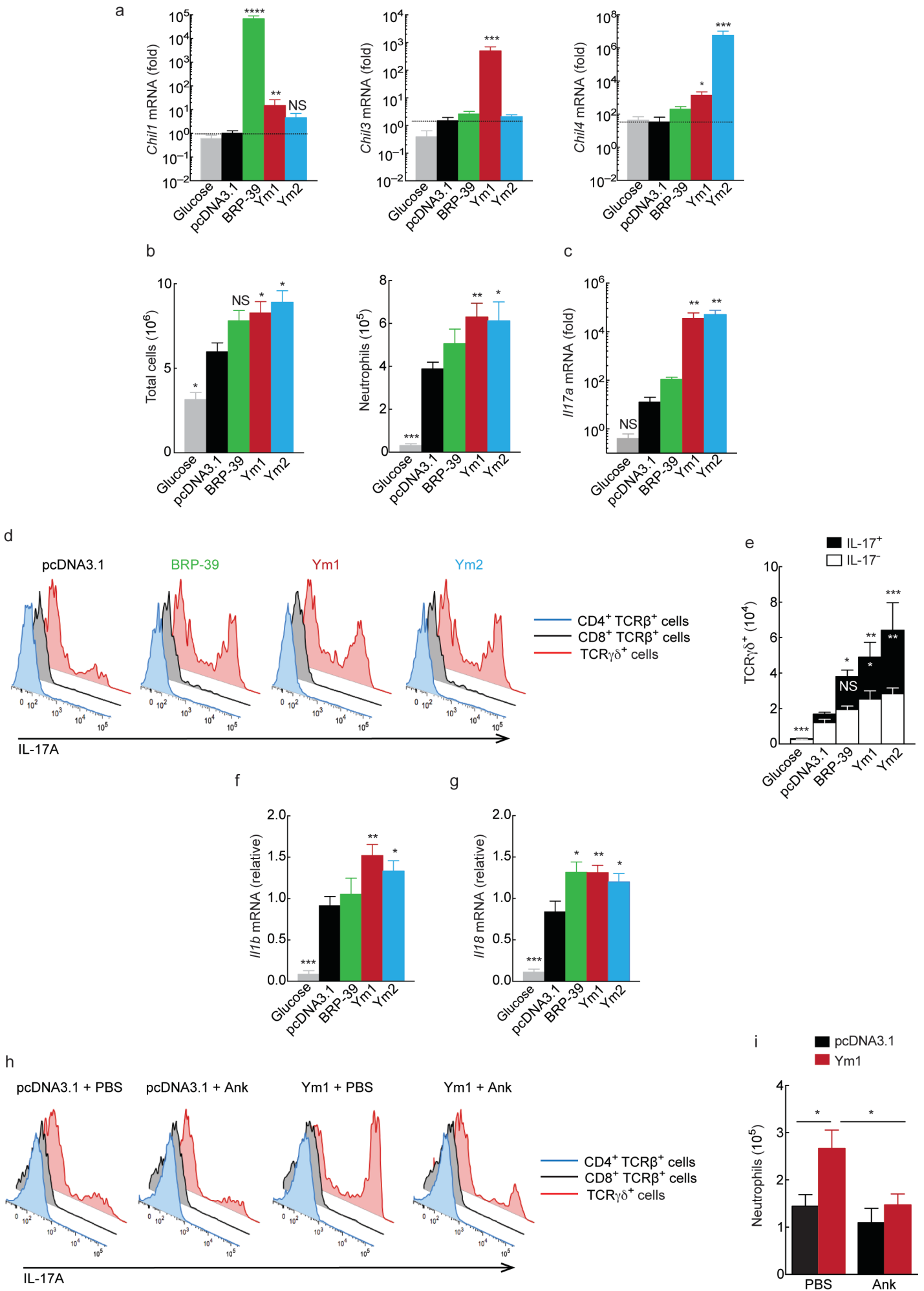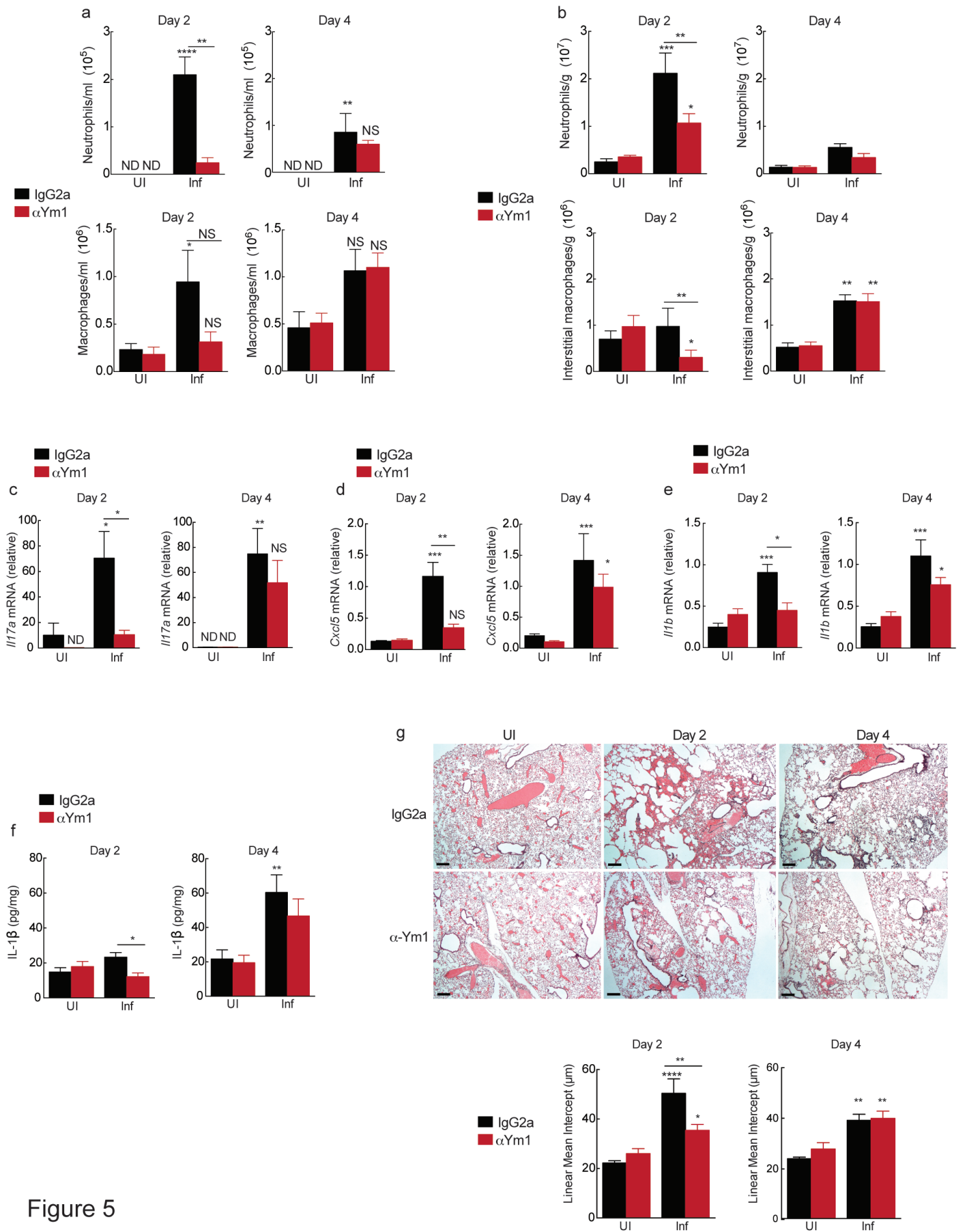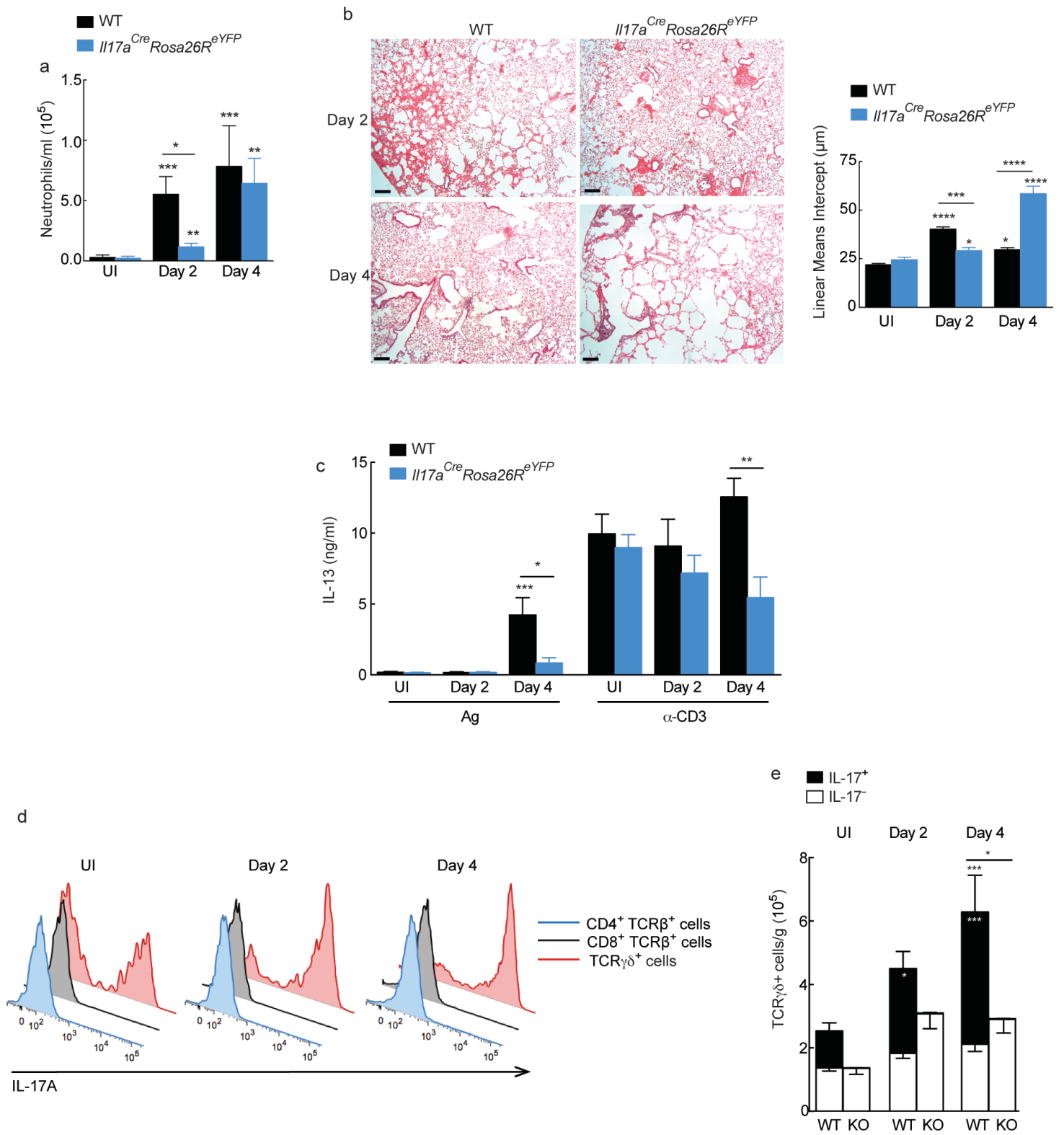*Chil4* naive — *Chil4* infected
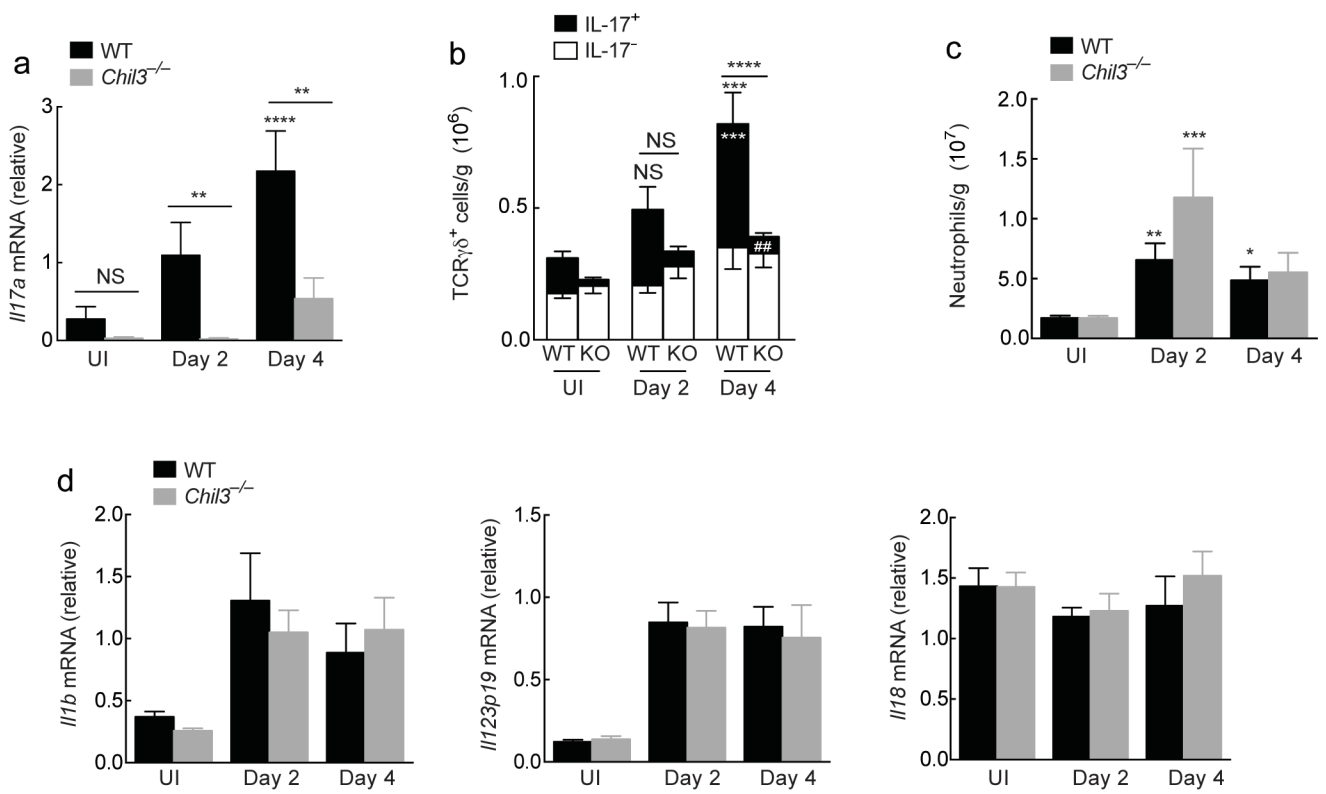
PBS

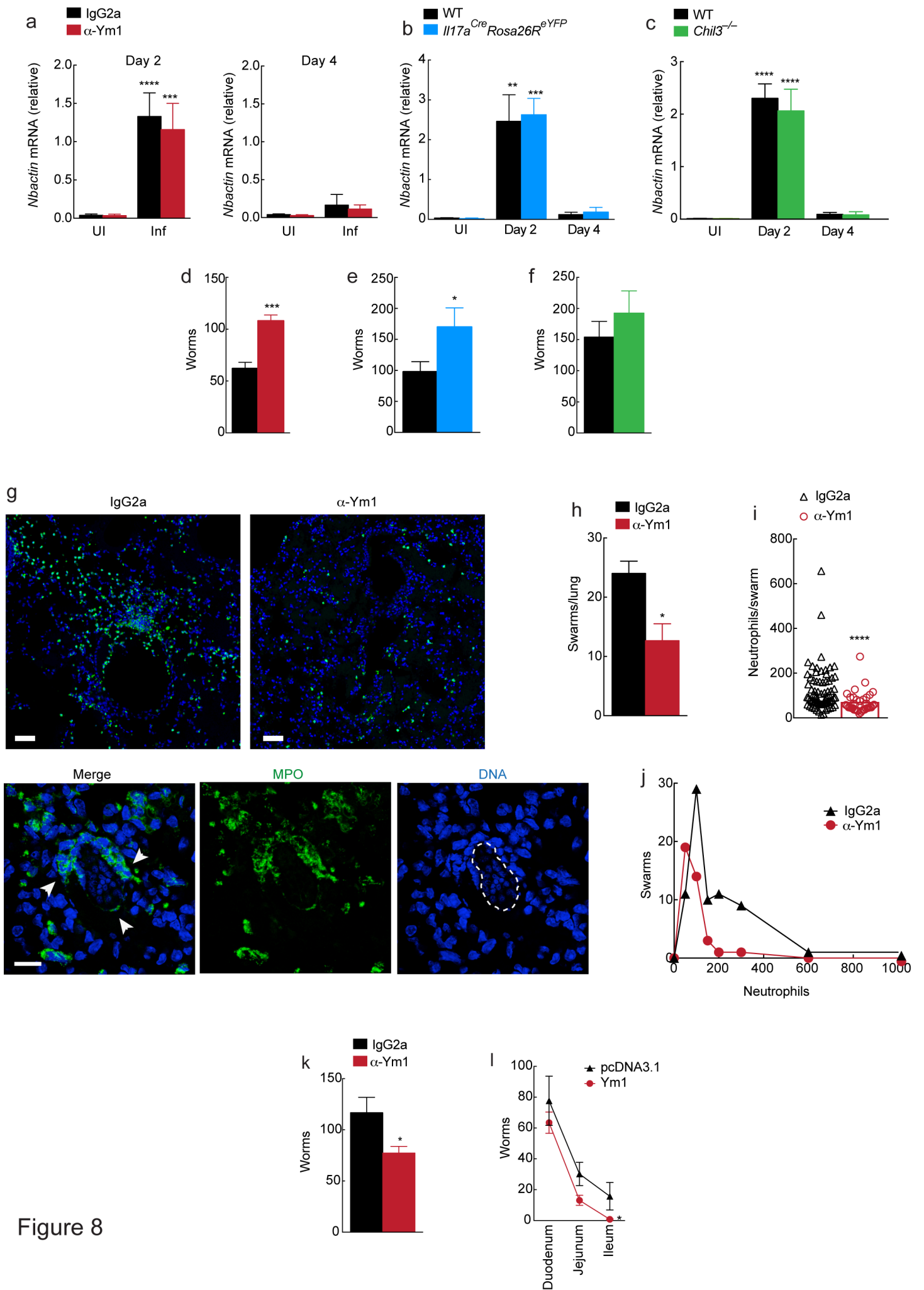OVA

Figure 1

Figure 2

a

b

c
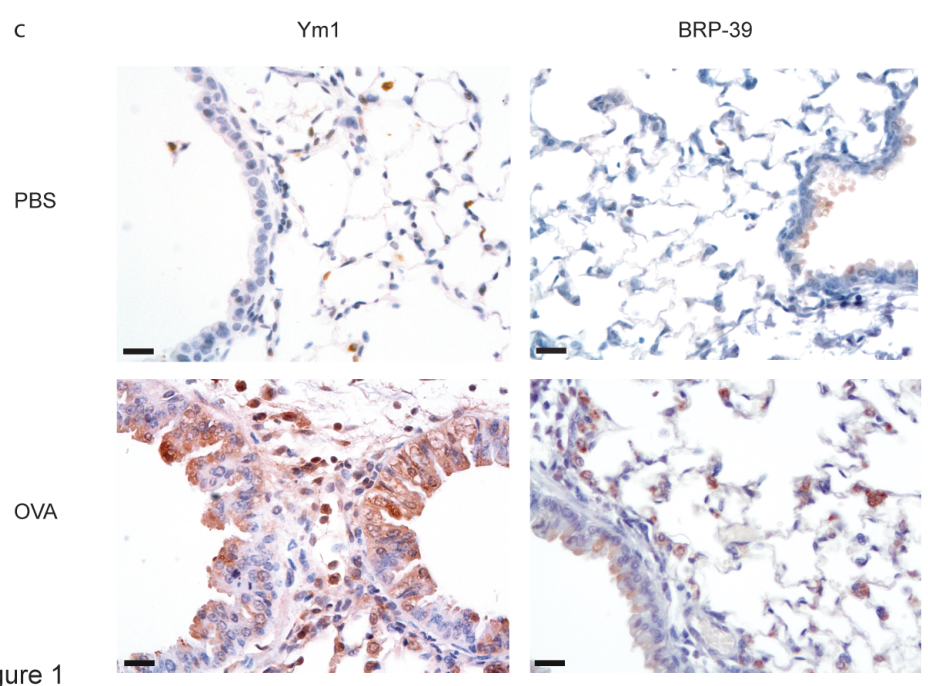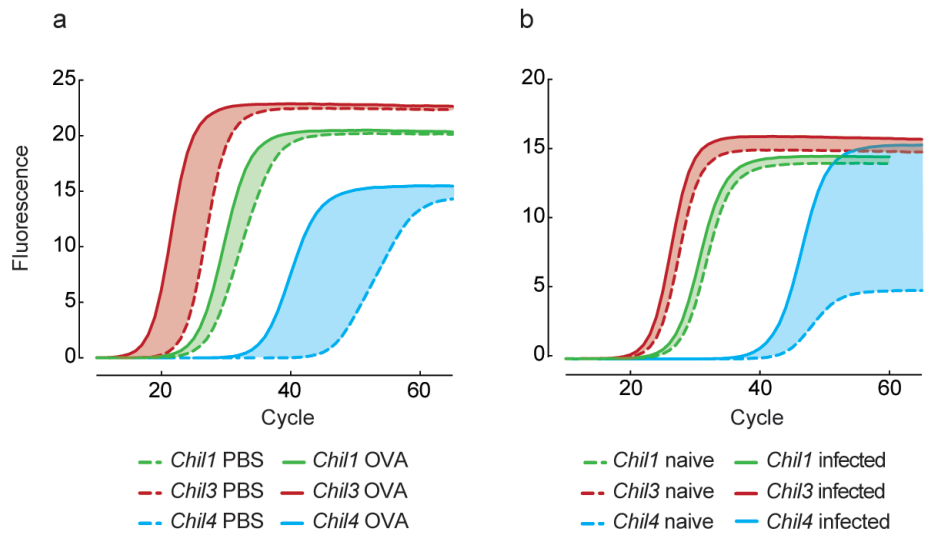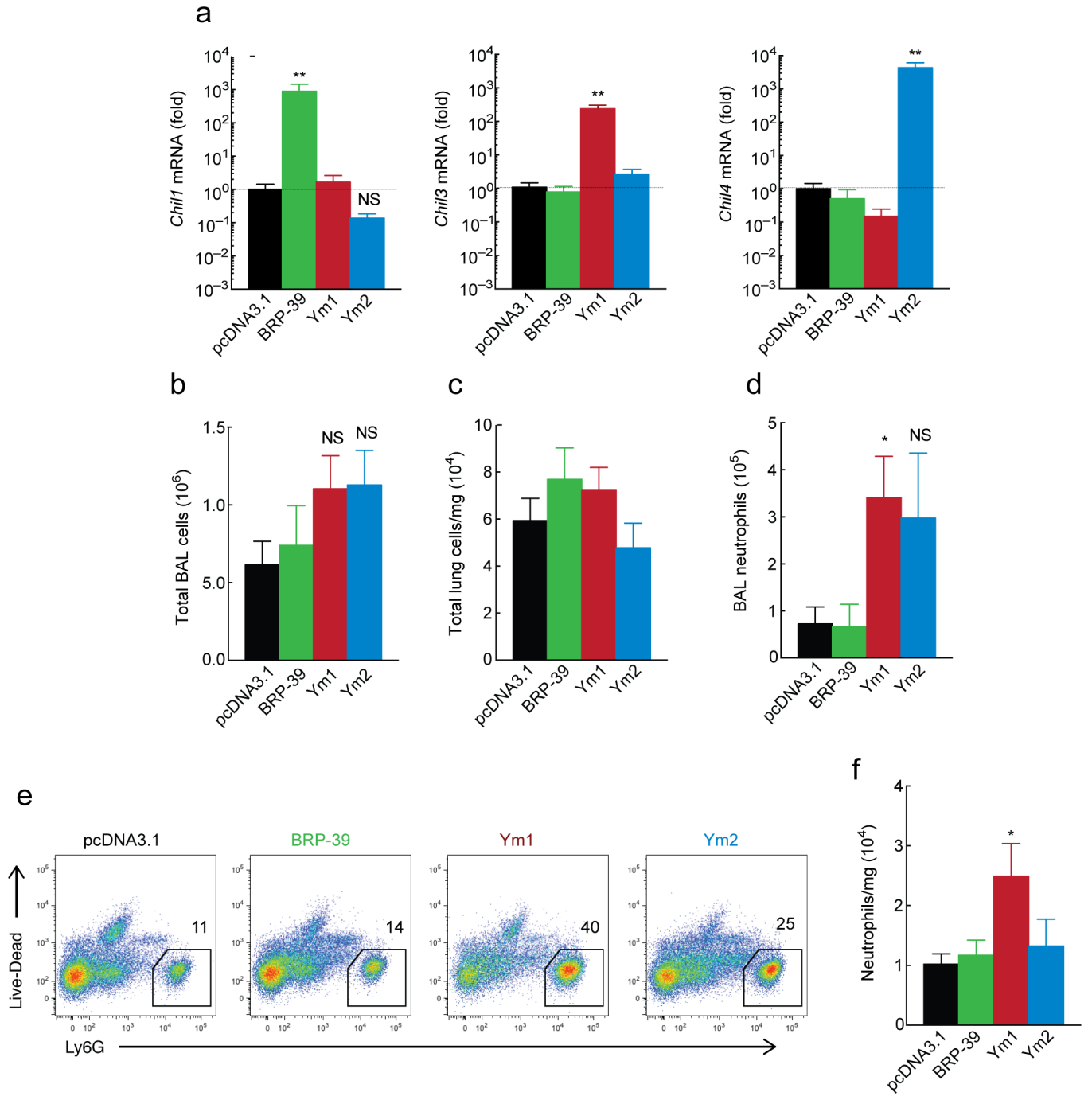
Figure 3

Figure 4

Figure 5

Figure 6

Figure 7

Figure 8